Anharmonic decay and the propagation of phonons in an isotopically pure crystal at low temperatures: Application to dark-matter detection

Humphrey J. Maris
Department of Physics, Brown University, Providence, Rhode Island 02912

Shin-ichiro Tamura
Department of Engineering Science, Hokkaido University, Sapporo 060, Japan
(Received 21 October 1991; revised manuscript received 3 April 1992)

We consider the propagation and anharmonic decay of high-energy phonons introduced into a perfect dielectric crystal at low temperatures. The phonon-decay rate is calculated for an fcc model with central forces between nearest neighbors. We give an approximate relation between the parameters entering into this model and the experimentally known properties of real crystals. A discussion is given of the range of wave vectors over which slow transverse phonons are stable against anharmonic decay. These results are relevant to the design of experiments to detect dark matter via the study of the phonons excited in a crystal when a dark-matter particle scatters off a nucleus. We discuss the primary phonon production mechanism and the possibility that there is an anisotropy of the phonon flux that is related to the direction in which the nucleus recoils.

I. INTRODUCTION

In this paper we consider what happens when high-energy phonons are introduced into an ideal crystal (isotopically pure and free of defects) at low temperatures. This problem is of considerable current interest because of recent attempts to develop phonon-based detectors of dark matter.[1,2] In these proposed detectors a dark-matter particle will scatter off a nucleus in a dielectric crystal that is at a temperature below 1 K. The recoiling nucleus will generate phonons in the crystal, and these will be sensed by an array of detectors at various points on the crystal surface. To consider in more detail what happens in this type of experiment it is useful to divide the detection process into the following steps.

(1) The recoiling nucleus loses energy via collisions with other atoms in the crystal. A wide variety of phenomena may occur as part of this process,[3] and these phenomena are dependent on the recoil energy, the nature of the interatomic forces, and the crystal structure. As part of this process some numbers of the atoms in the crystal may end up in positions removed from their original sites in the crystal.

(2) At the end of this stage a large number of high-energy phonons are produced ("primeval phonons"). Without considering the details of step (1), it seems likely that because a large amount of energy is available, excitation will occur all across the phonon spectrum. Thus the average phonon energy at this stage would be on the scale of the Debye energy, which for silicon is 660 K, or roughly 60 meV.

(3) Even in a perfect crystal the majority[4] of these phonons are unstable against anharmonic decay (lifetimes 10–100 psec). Thus, the distance that they can travel before decaying is very small compared to the size of the crystal. However, after each decay process their lifetime becomes longer by a large factor because the anharmonic decay rate varies approximately as E^5. When a sufficient number of decays has occurred the phonon mean free path becomes as large as the crystal dimensions. The phonons then propagate ballistically until they reach the surface of the crystal. For a crystal of dimensions of the order of centimeters the typical energy of the phonons at this stage is in the range 20–30 K, or 2–3 meV.

(4) At the end of stage (3) some fraction of the phonons will enter whatever detectors are placed at the surface of the crystal and will produce a signal. The phonons that do not manage to enter the detecting device (or devices) will bounce around the crystal. Calculations show that because of the rapid dependence of the anharmonic decay rate on the phonon energy the intrinsic anharmonic decay rate will not thermalize the phonon distribution on a typical experimental time scale.[5] In addition, elastic scattering of the phonons at the surface of the crystal does not lower the phonon energy. However, it is possible that interaction with defects in the crystal, some types of defects at crystal surfaces, or with electrons in metallic films deposited onto the crystal surface may cause a degree of thermalization. Regardless of their energy the phonons will continue to enter the detecting device and will give a signal.

(5) Eventually the phonons escape from the crystal via whatever heat links exist to the outside world.

The magnitude of the detected signal [either at the end of stage (3) or while the phonon remnants are bouncing around the crystal in stage (4)] can be used as a measure of the energy of the recoiling nucleus. From the arrival time of the phonons at different detectors at the end of stage (3) it should be possible to determine where in the crystal the scattering took place. In addition, it would be a great advantage if the detected phonon signals could be analyzed to determine the direction of recoil of the nucleus. Knowledge of the recoil direction would provide a powerful technique to reduce the interference from the

internal radioactivity of the crystal. It is reasonable to believe (see discussion in Sec. II) that the phonons initially generated by the recoil [i.e., the "primeval phonons" in (2) above] have *some* degree of anisotropy with respect to the recoil direction. By anisotropy we mean anisotropy in addition to the usual phonon-focusing effects. For example, if the nucleus recoils along the z axis the intensity of the generated phonons propagating along the [001] and [00$\bar{1}$] may differ from the intensities along [100], [$\bar{1}$00], [010], and [0$\bar{1}$0]. In a crystal containing a mixture of different isotopes all phonons except those of very low frequency undergo strong-elastic scattering, and the anisotropy in the phonon distribution will probably be lost before the phonons reach the detectors. However, in high-quality crystals of isotopically pure material it is possible that some part of the anisotropy of the primary phonons will persist, and so the track direction can be determined.

As already mentioned, most high-energy phonons (energy E comparable to $k_B\Theta_D$, Θ_D = Debye temperature) decay very quickly into lower-energy phonons as a result of anharmonic processes. These product phonons may then undergo further decays. Since the rate Γ of decay by these anharmonic processes[6] increases rapidly with increasing phonon energy E, the lifetime of the product phonons is much longer than the lifetime of the original phonon. As a consequence of this large increase in lifetime, Kazakovtsev and Levinson[7,8] (KL) have proposed that the evolution of the phonon distribution should be viewed as a "succession of generations." According to their picture the largest part of the distance from the source to a detector is always traveled by the last generation, because this generation has the largest lifetime. KL refer to propagation under these conditions as "quasiballistics." They predict[9] that the phonons will arrive at a detector a distance L from the source at a time which is longer than the time $t_B \equiv L/v$ (v = phonon velocity) that would be taken by freely propagating ballistic phonons by some factor a. The factor a is of the order of unity but, of course, $a > 1$. The time aL/v is the *average* time for the phonons to reach the detector; it is predicted[9] that there will be a broad and smooth distribution of arrival times. The KL theory assumes implicitly that all phonons are able to decay, whereas in fact there is a part of the phonon spectrum that is stable. In addition, the effect of phonon focusing[10] is not considered. In this paper we discuss the effects that stable phonons and phonon focusing have on the phonon propagation and we arrive at a picture substantially different from KL.

II. GENERATION OF PHONONS

In this section we give a qualitative discussion of the primary generation of phonons by dark matter in a crystal in order to motivate the subsequent discussion of phonon decay. A review of dark-matter particle candidates has been given by Primack *et al.*[11] For the majority of these candidates the interaction is with the nuclei in the crystal, rather than with atomic electrons. The amount of energy transferred to the nucleus is expected to be of the order of 1 keV. The velocity of the nucleus is smaller than the velocity of the atomic electrons, and thus as a first approximation the atom recoils as a unit. The recoil energy is significantly larger than the energy $E_{\rm dis}$ typically required to displace an atom from a lattice site. In Si, for example, $E_{\rm dis}$ is between 11 and 22 eV, depending on the direction of recoil.[12]

Some of the physical considerations relevant to the phonon generation are as follows.[13]

(1) For very low energy no permanent atomic displacement will occur and the momentum $\mathbf{p}$ of the recoiling atom will be sufficiently small that the subsequent motion can be well approximated by lattice dynamics in the harmonic approximation. Then it is straightforward to show based on classical lattice dynamics[14] that the energy appearing in the phonon mode of wave vector $\mathbf{k}$ and polarization j is

$$E_{\mathbf{k}j} = (\mathbf{p}\cdot\mathbf{e}_{\mathbf{k}j})^2/(2NM) , \tag{1}$$

where N is the number of atoms in the crystal, M is the atomic mass, and $\mathbf{e}_{\mathbf{k}j}$ is the polarization vector of the phonon mode. This formula holds for Bravais lattices and also for crystals of the diamond structure (e.g., C, Si, and Ge). When this formula holds longitudinal phonons are generated most strongly in the forward and backward directions along the recoil direction. Transverse phonons are radiated most strongly perpendicular to the track, and these phonons are polarized parallel to the recoil direction. Note that the phonon distribution should have inversion symmetry, so that the intensity in the forward and backward directions relative to the track are equal. It is clear that Eq. (1) is valid only at very low energies, i.e., much less than the energy required to produce atomic displacement. Thus, in silicon the energy would probably have to be ≤ 1 eV.

(2) When the energy is higher anharmonic effects become important. As a very simple model we have considered what happens for a linear chain of particles (typically $\sim$200 atoms) interacting via a Lennard-Jones potential of the form

$$U(r) = \epsilon[(\sigma/r)^{12} - 2(\sigma/r)^6] , \tag{2}$$

where $U(r)$ is the potential when the atomic separation is r, ϵ is the depth of the potential well, and σ is the range. In the simulations all atoms are initially at rest in their equilibrium positions except the atom at the midpoint of the chain which is given a recoil velocity v_0. The interatomic spacing is slightly less than σ because of next-nearest-neighbor interactions. Starting from this configuration we time develop the equations of motion of the atoms until most of the energy has left the region near to the recoil atom. Then we determine the fractions f_+ and f_- of the energy that propagate in the forward and backward directions. Results are shown in Fig. 1. When the energy of recoil becomes comparable to or greater than ϵ, most of the energy propagates in the forward direction, i.e, $f_+ \approx 1$. Examination of the detailed results from the computer simulations shows that to a good approximation in this range of recoil energies the disturbance in the chain can be divided into two separate parts. The first part consists of waves propagating away

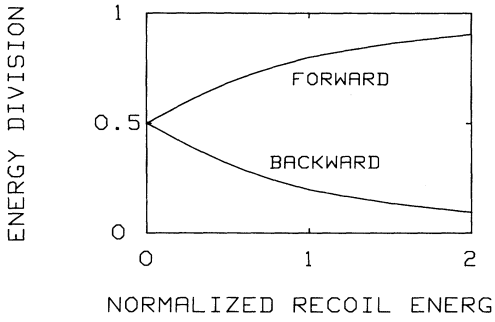

FIG. 1. Fractions of energy propagating in the forward and backward directions in a linear chain. The recoil energy is measured in units of the strength ϵ of the interatomic potential [see Eq. (2)].

from the recoil point in the forward and backward directions. The spatial form and velocity of these waves is nearly independent of recoil energy. The front of these disturbances propagates at the speed v_{sound} of low-amplitude sound in the chain equal to $8.6\sqrt{\epsilon/M}$. The second part of the disturbance is a solitary wave[15] propagating in the direction of recoil with a speed greater than v_{sound}. As the recoil velocity increases, more and more of the recoil energy appears in this solitary wave, and hence a larger fraction of the energy propagates in the forward direction. In Fig. 2 we show the distribution of particle velocities in the chain when the recoil energy is 2ϵ. This distribution is for a time $t=2\sigma\sqrt{M/\epsilon}$ after the recoil.

(3) In higher dimensions several extra physical effects enter, and these have a large effect on the symmetry of the primary phonon generation. It is likely that the physics will be quite different depending on the crystal structure and the nature of interatomic bonding. Permanent atomic displacements of various types can be produced, e.g., Frenkel pairs, voids, disordered regions. The region in which these occur may be surprisingly large. This is because energy can be efficiently transported in specific

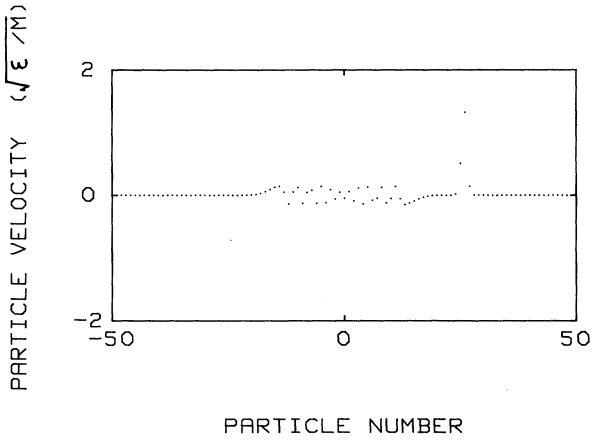

FIG. 2. Velocity distribution of particles in a linear chain. At time zero all particles were at rest in their equilibrium positions except for particle 0 at the midpoint of the chain. The recoil energy of this particle was 2ϵ.

crystal directions by weakly damped excitations that carry energy and mass. These excitations have been called "focusons" and "dynamic crowdions."[3] These effects have been studied by several workers by means of molecular-dynamics simulations. However, the primary interest has been in determining the nature of the damage produced as a function of the recoil energy and the type and strength of the bonding in the crystal.[3,16] We are unaware of any calculations of the phonon radiation produced in these processes. To perform a realistic calculation for a covalently bonded crystal, such as Si or Ge, is extremely difficult because of the complexities of the interatomic potential, particularly the contributions from terms involving the angular positions of neighboring groups of atoms.[17]

We have investigated the phonon generation in two dimensions in a very simple system. We took the same interatomic potential as in Eq. (2) and in the equilibrium configuration the atoms formed a hexagonal lattice. The simulations started with all atoms at rest at their equilibrium positions except for the atom at the center of the array which was given a recoil velocity v_0 in a direction θ relative to one of the hexagonal axes. For small values of v_0 the energy of recoil appears as low-amplitude waves propagating away from the origin, with an equal amount of energy going in the forward and backward directions as expected according to Eq. (1). For larger v_0 there appear, in addition to these waves, excitations akin to the solitons found in one dimension.[18] However, there are some important differences as follows.

(a) The excitations are disturbances that are confined to rows of atoms that start at the atom at the origin (i.e., the atom that is given the recoil velocity) and radiate outward along the principal axes of the hexagonal lattice (Fig. 3). If the direction of recoil coincides with one of these directions there will be only one excitation produced and naturally it will propagate along this same direction. For an arbitrary recoil direction $\hat{\mathbf{n}}$ two excitations are usually produced which travel along the two hexagonal axes closest to $\hat{\mathbf{n}}$.

(b) The velocity distribution of the atoms in these rows are very similar to the velocity distribution shown in Fig. 2 for the linear chain. The velocity v_s of the excitation increases with v_0. In units of $\sqrt{\epsilon/M}$, v_s has the values 22, 34, and 54 when v_0 is 5, 10, and 20, respectively.[19]

(c) In contrast to the result found in one dimension, these excitation are attenuated as they propagate, and are thus not true solitons. At any stage of propagation of the excitation we can measure its amplitude in terms of the maximum velocity $v_{\max}$ that an atom lying in the row reaches as the excitation passes by. This velocity decreases as the excitation propagates and the fractional decrease of $v_{\max}$ per lattice spacing decreases rapidly as $v_{\max}$ increases. This damping is the analog of Cerenkov damping and can occur because the excitation travels faster than the velocity of sound. Phonon energy is radiated by the excitation into a cone of angle

$$\alpha=\sin^{-1}(v_{\text{sound}}/v_s) \tag{3}$$

with the cone axis on the propagation direction. In the two-dimensional model considered the velocity of longi-

tudinal sound is approximately $11\sqrt{\epsilon/M}$.

Within this model the symmetry of the generated phonons thus varies greatly according to the recoil energy. One can divide the range of energy as follows.

(i) For a recoil energy smaller than the strength ϵ of the potential the energy radiated in the forward and backward direction is equal. There may, however, be more (or less) energy radiated perpendicular to the recoil direction than in the forward and backward directions [see Eq. (1)].

(ii) For higher energies solitonlike excitations are generated but their velocity does not greatly exceed the velocity of sound. Consequently, the angle α is large and most of the phonon radiation goes approximately into the forward direction.

(iii) Finally, at sufficiently high-recoil energies the soliton velocity becomes much larger than v_{sound}. The angle α then becomes small. In this regime there is a small forward-back anisotropy (in favor of the forward direction), but the radiation of energy is strongest in the plane perpendicular to the recoil direction.

In our two-dimensional model the binding energy per atom is $E_{\text{bind}} \sim 6\epsilon$. The boundaries between the different regimes are not sharp but the simulations we have performed suggest that the transition from (i) to (ii) occurs at a recoil energy of around $E_{\text{bind}}/10$, and from (ii) to (iii) at about $3E_{\text{bind}}$. Thus, if the recoil energy is in the range around 1 keV, one is in regime (iii).

An interesting feature of the results is that the motion of the system after an atom is given a recoil velocity is not random but is "deterministic." Thus, if the direction or the energy of the recoil is changed by a small amount the ensuing motion of the nearby atoms is changed only slightly. This is in contrast to what would be expected for chaotic motion where a slight change in the initial conditions would cause the details of the resulting motion to be substantially different.

The model we have just described may give a reasonable qualitative description of phonon generation in monatomic close-packed crystals in which the interatomic potential can be approximated by the Lennard-Jones form Eq. (2).[20] These crystals include the inert gas solids He, Ne, Ar, Kr, and Xe. We have also made a preliminary investigation of the dynamics of systems composed of two types of atom with differing mass interacting via a Lennard-Jones potential. In one dimension we again find solitons provided that the recoil velocity is sufficiently large, but whether the damping is strictly zero, or merely very small has not yet been determined. We are currently performing numerical simulations to determine whether the same type of effect (i.e., solitons) occur in alkali-halide crystals, such as NaF. In alkali-halide crystals the interatomic potential can be taken to be the sum of an ionic contribution together with a repulsive term between nearest neighbors. In crystals with covalent bonding (e.g., Si, Ge, GaAs) that have a more open structure the physics is probably quite different, since rows of atoms with close spacing do not exist and the openness of the structure provides opportunities for a quasiparticle to break up. Consequently, the motion in such systems will probably be chaotic, as distinct from deterministic (see above discussion). For these materials we are not aware of calculations of even the final atomic displacement patterns for energies in the range of interest here (around 1 keV), let alone details of the phonon radiation field. Estimates of the range of a recoiling particle based on the Lindhard model are given in the review of Smith and Lewin.[21] This model does not take into account the possibility of the formation of solitons.

III. PHONON DECAY PROCESSES

In this section we consider the anharmonic decay of phonons in a perfect crystal at $T=0$ K, with particular emphasis on the variation of the decay rate with the phonon wave vector and polarization.

A. fcc lattice

The simplest model to consider is an fcc lattice of atoms of mass M interacting by nearest-neighbor central forces. For this model several aspects of the anharmonicity have been studied by Maradudin and co-workers.[22,23] The model is attractive because the harmonic interactions are completely specified by the value ϕ'' of the second derivative of the interatomic potential at the nearest-neighbor distance. This quantity can be related to the bulk modulus B and the second-order elastic constants C_{ij} via the equations

$$B = \frac{4\phi''}{3a_0} , \tag{4}$$

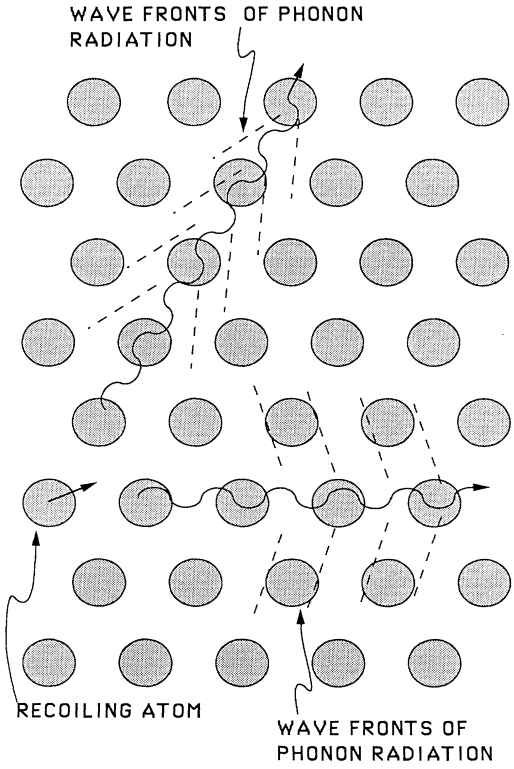

FIG. 3. Generation of phonons (denoted by the wavy lines) via the production of "focusons."

$$C_{11}=2C_{12}=2C_{44}=\frac{2\phi''}{a_0} , \tag{5}$$

where a_0 is the lattice parameter, i.e., the nearest-neighbor distance times $\sqrt{2}$. The density ρ of the crystal is equal to $4M/a_0^3$. The phonon dispersion relation is shown in Fig. 4.

The cubic anharmonicity is specified by the third derivative ϕ''' of the potential. It can be shown[22] that for temperatures near the Debye temperature or higher the volume thermal expansions coefficient α is

$$\alpha=-\frac{3\sqrt{2}\,k_B\phi'''}{4\phi''^2 a_0} . \tag{6}$$

Thus, the Grüneisen constant is

$$\gamma=\frac{\alpha B}{C}=-\frac{\phi''' a_0}{6\sqrt{2}\,\phi''} , \tag{7}$$

where C is the specific heat per unit volume. From these results it follows that we can uniquely determine the microscopic parameters in the model (ϕ''', ϕ'', M, and a_0) if we require that these parameters be consistent with the values of the four quantities γ, ρ, B, and M. In Table I we list values of these quantities for several crystals. For LiF, NaF, Si, and Ge we have used the experimentally determined value[24] for the thermal expansion coefficient at temperatures in the vicinity of Θ_D to determine an approximate value of γ via Eq. (7). For Ar, Kr, and Xe the high-temperature value of the Grüneisen constant is around 2.7.[24] For Ne one cannot measure the thermal expansion at a temperature near to Θ_D, since the melting temperature is less than Θ_D. However, by the law of corresponding states the value of γ should be the same in all Lennard-Jones solids (at least ignoring quantum effects), and so we use the value 2.7 also for neon.

It follows from the general expression for the three-phonon anharmonic decay rate[23] $\Gamma(\mathbf{k}j)$ (the inverse of the phonon decay time) that we can express this quantity in the form

$$\Gamma(\mathbf{k}j)=\Gamma_0 G(\mathbf{k}j) , \tag{8}$$

where

$$\Gamma_0=\frac{\hbar\gamma^2\rho^{2/3}}{M^{5/3}} \tag{9}$$

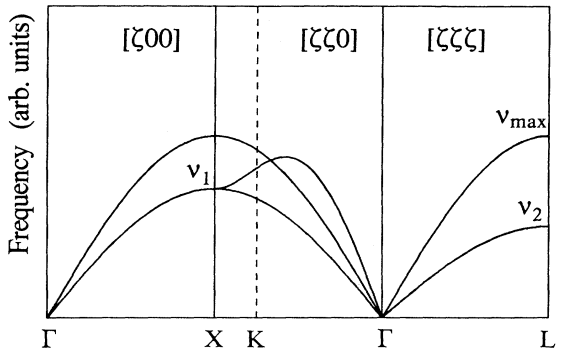

FIG. 4. Dispersion relation for phonons propagating in the principal directions according to the fcc model. The maximum frequency ν_{max} is $(2\phi''/\pi^2 M)^{1/2}$, $\nu_1=\nu_{max}/\sqrt{2}$, and $\nu_2=\nu_{max}/2$.

and G is a dimensionless function. We have calculated G for phonons propagating in the principal crystallographic directions and the results[25,26] are shown in Fig. 5.

For frequencies small compared to the Debye frequency the decay rate must vary as the frequency ν to the fifth power, as was shown by Herring.[27] Thus, we can write the decay rate as

$$\Gamma(\mathbf{k}j)=\Gamma_0(\nu/\nu_{max})^5 g(\hat{k}j) , \tag{10}$$

where $g(\hat{k}j)$ is a dimensionless function of the wave-vector direction $\hat{k}$ and the polarization. Numerical results for $g(\hat{k}j)$ with $\hat{k}$ lying in {100}- and {110}-type planes are shown in Fig. 6. As an alternative expression of the result we can write

$$\Gamma(\mathbf{k}j)=\Gamma_1\nu_{THz}^5 g(\hat{k}j) , \tag{11}$$

where ν_{THz} is the frequency in units of THz, and

$$\Gamma_1=\frac{\pi^5 2^{5/6}10^{60}}{3^{5/2}}\frac{\hbar\gamma^2\rho^{3/2}}{B^{5/2}} . \tag{12}$$

This result is obtained by expressing ν_{max} in terms of B, ρ, and M. Values of Γ_1 are included in Table I.

For the subsequent discussion it is important to know which phonons are unable to decay. The possibility that some phonons are unable to decay as a result of the requirements of conservation of energy and momentum was pointed out by Orbach and Vredevoe,[28] and has since

TABLE I. Grüneisen constant γ, density ρ, mass M, and bulk modulus B for several crystals. Γ_0 and Γ_1 are constants entering into the calculation of the phonon decay rate [Eqs. (8) and (11)].

	γ	ρ g cm^{-3}	M 10^{-24} g	B 10^{10} dyne cm^{-2}	Γ_0 10^{12} s^{-1}	Γ_1 10^6 s^4
Ne	2.7	1.51	33.5	1.1	0.29	38000
Ar	2.7	1.77	66.3	3.0	0.10	4000
Kr	2.7	3.09	139.1	3.6	0.044	5900
Xe	2.7	3.78	218.0	3.6	0.024	7800
LiF	1.6	2.65	43.1	70	0.097	1.0
NaF	1.5	2.85	69.7	52	0.040	2.1
Si	0.58	2.33	93.3	99	0.0032	0.045
Ge	0.72	5.32	241.0	77	0.0018	0.46

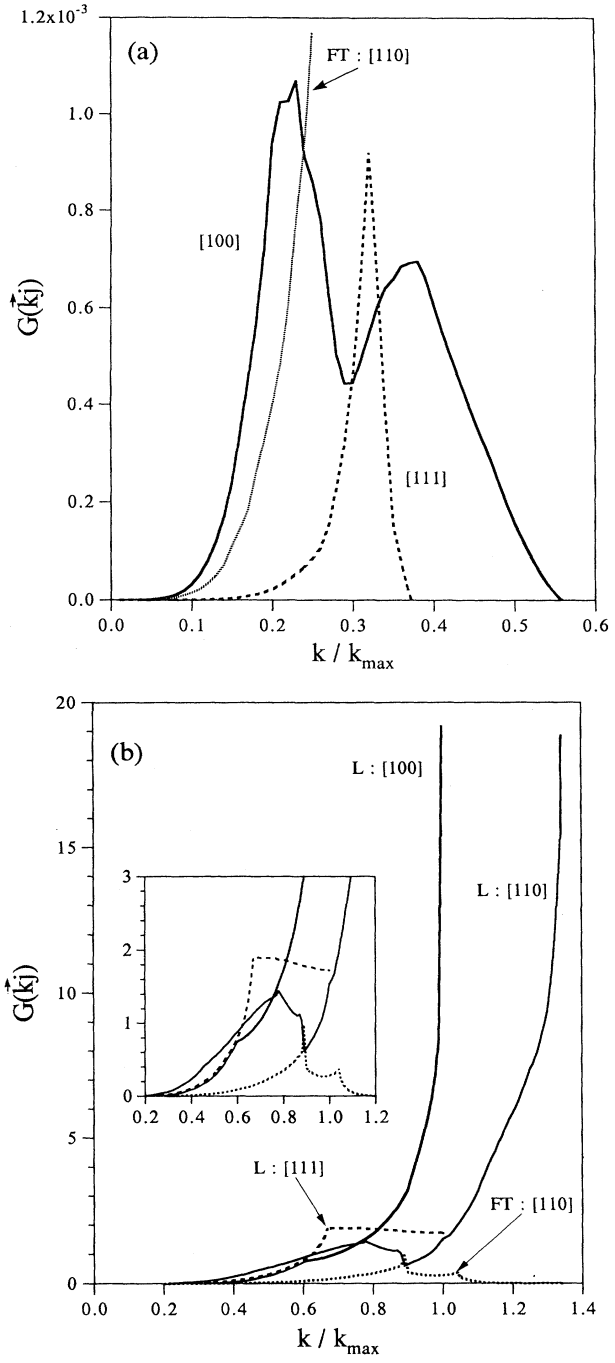

FIG. 5. Decay rates for phonons propagating in the principal directions of an fcc crystal. The quantity plotted is the dimensionless decay rate defined in Eq. (8). k_{max} is the zone-boundary wave number for each direction considered. (a) Decay of slow transverse ST phonons. For [111] propagation the decay only occurs via the ST→ST+ST process. In the [110] direction ST phonon decay cannot occur. (b) Decay of longitudinal L and fast transverse FT phonons. Inset is a view of the results on an expanded scale. The results for the [110] direction have been continued out beyond the zone boundary (K) to the X point in the second zone ($k/k_{max}=\frac{4}{3}$). For the [100] and [111] directions there is no distinction between FT and ST phonons, so for FT phonons the results of (b) apply.

been discussed in more detail by others.[29–32] Stable phonons all come from the slow transverse (ST) branch of the phonon spectrum. In Fig. 7 we show the regions of the (100) and (110) planes containing the wave vectors of ST phonons that cannot decay. These results are calculated using a cubic mesh of points in the first Brillouin zone with spacing such that there are 100 points along the k_x axis from the zone center to the zone boundary. For ST phonons of low frequency the stable phonons have $\hat{k}$ lying within a certain range of directions, and this range is shown in Fig. 8.

Figures 7 and 8 show the phonon wave vectors for which ST phonons can decay by the three-phonon process. If one were to consider higher-order decay processes such as the four-phonon process the region in which phonons can decay may be somewhat larger. However, it follows from the results of Lax *et al.*[30] that the size of the

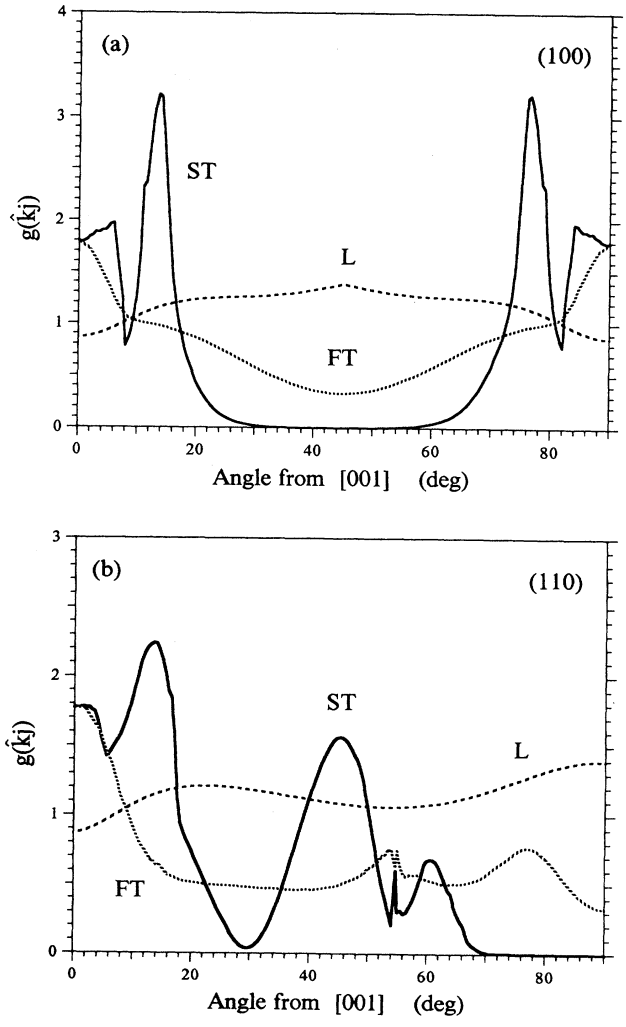

FIG. 6. The rate of decay of low-frequency phonons as a function of the direction of propagation. The decay rate is $\Gamma(\mathbf{k}j)=\Gamma_1 v_{THz}^5 g(\hat{\mathbf{k}}j)$ where Γ_1 is given by Eq. (12) and Table I, and ν_{Thz} is the frequency measured in THz. (a) (100) plane and (b) (110) plane. These calculations are for the fcc model described in the text.

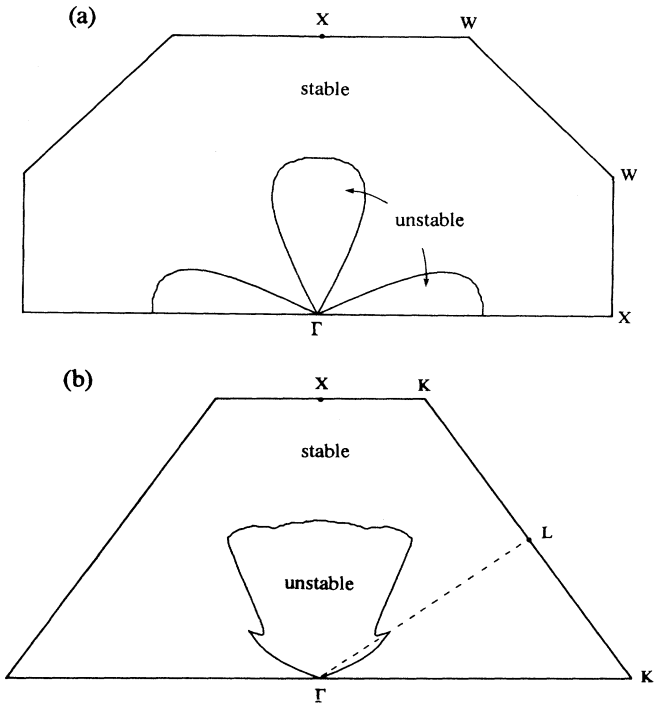

FIG. 7. Regions of the (a) (100) and (b) (110) planes in which slow transverse phonons are stable against anharmonic decay by the three-phonon process. These calculations are for the fcc model described in the text.

unstable region cannot be greatly increased. They point out that at least one of the decay products must always have a velocity greater than that of the original phonons. Hence, neither ST phonons from the dispersive region nor ST phonons of small wave number that propagate in directions where the phase velocity is small can decay, regardless of the order of the process.

B. Silicon

Phonon decay in silicon has been studied previously by several authors. Narasimhan and Vanderbilt[33] have calculated the decay rates for optical phonons with **k** along symmetry directions. It appears that all of the optical phonons have nonzero decay rates. Calculations of the lifetime of acoustic phonons have been restricted to results for the decay rates of low-frequency phonons. Then one can use experimentally measured values of the third-order elastic constants to calculate the three-phonon matrix element, and it is therefore not necessary to construct a detailed model for the interatomic potential. This has been done by Berke *et al.*[32] for the longitudinal (L) and fast transverse (FT) branches. For the ST branch we have calculated the region of momentum space in which phonons are unable to decay. These results are shown in Figs. 9 and 10. The calculations in Fig. 9 are based on the model of the lattice dynamics of silicon developed by Tamura *et al.*,[34] and the mesh of points was the same as that used to produce Fig. 7. The results for low-energy phonons in Fig. 10 use the same elastic constants as in Ref. 32. The region in **k** space in which ST phonons are unstable in silicon is much smaller than the corresponding region for the fcc model. This is because in silicon the dispersion curve for the ST branch exhibits a marked flattening toward the Brillouin zone boundary.

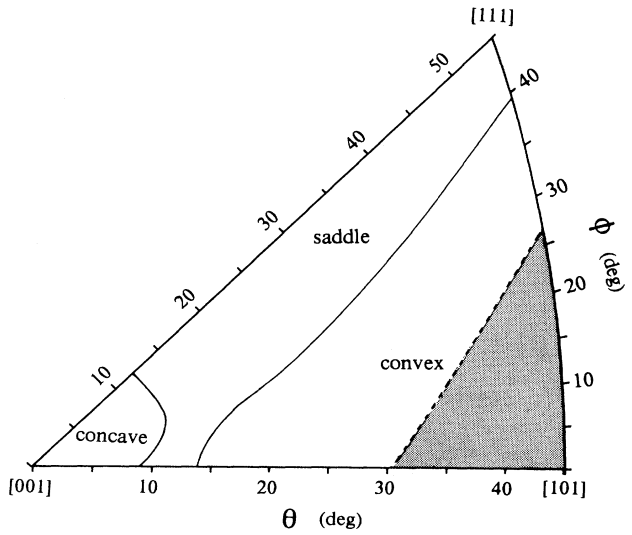

FIG. 8. The shaded region shows the range of directions of the phonon wave vector for which low energy ST phonons are stable against anharmonic decay. These calculation are for the fcc model described in the text.

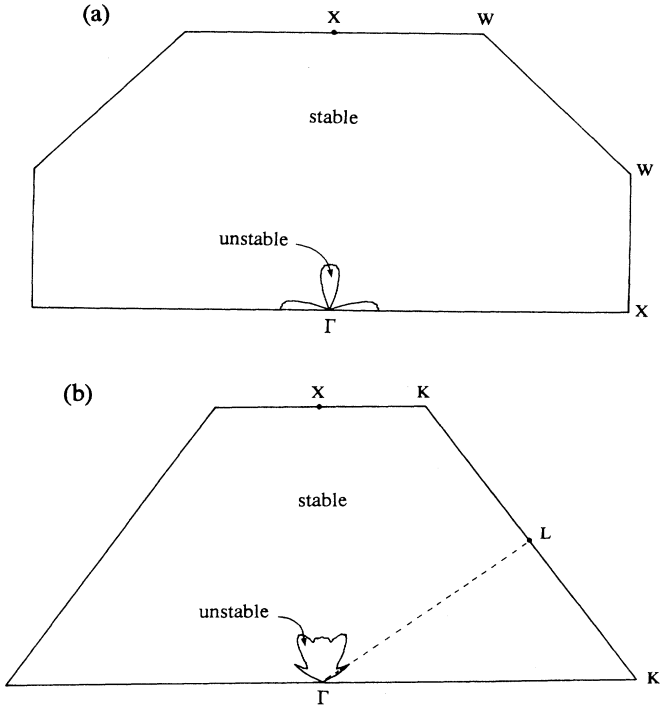

FIG. 9. Regions of the (100) and (110) planes in which slow transverse phonons are stable against anharmonic decay by the three-phonon process. These calculations are for silicon using the model described in Ref. 33.

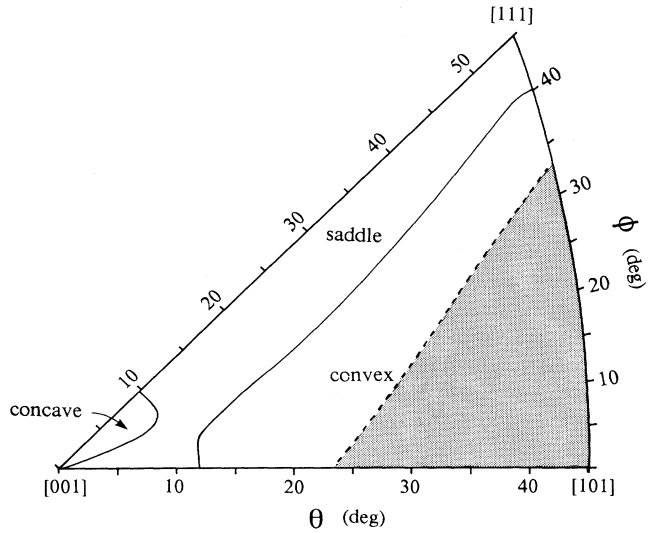

FIG. 10. The shaded region shows the range of directions of the phonon wave vector for which low-energy ST phonons are stable against anharmonic decay. These calculations are based on the measured elastic constants of silicon.

C. Conditions for phonon decay

The stable phonons discussed above exist because for certain values of $\mathbf{k}j$ it is impossible to find decay products $\mathbf{k}_1 j_1$ and $\mathbf{k}_2 j_2$ such that the conditions of energy and momentum conservation are satisfied. These conditions are

$$\omega(\mathbf{k}j)=\omega(\mathbf{k}_1 j_1)+\omega(\mathbf{k}_2 j_2)\ , \tag{13}$$

$$\mathbf{k}=\mathbf{k}_1+\mathbf{k}_2\ , \tag{14}$$

where ω is the angular frequency. To discuss the existence of solutions of these equations it is convenient to use a construction introduced by Herring[26] and shown in Fig. 11(a). Choose the $\mathbf{k}$ and j for the phonon whose decay is to be studied. This determines $\omega(\mathbf{k}j)$. Then choose some fixed value for the frequency for one of the phonons (say 1) produced in the decay. The set of phonons that have this frequency and a particular polarization j_1 lie on some surface S_1 in $\mathbf{k}$ space. Since the frequency of phonon 1 is fixed, the frequency of phonon 2 can be calculated from Eq. (13). One can now draw with origin at the point $\mathbf{k}$ a surface S_2 containing the wave vectors of all phonons that have the polarization j_2 and the required frequency. At any point of intersection of the surfaces S_1 and S_2 the equations of energy and momentum conservation are satisfied and so this corresponds to a possible decay process. S_1 and S_2 are surfaces of constant frequency (CF).

Using the Herring construction it is straightforward to show that acoustic phonons from the longitudinal and fast transverse branches can always decay. Optical phonons can also decay provided that the frequency of the optical modes is no more than twice the maximum frequency of the acoustic modes.[35] Thus, stable phonons can exist only from the slow transverse branch of the spectrum.

To analyze the stability of ST phonons we first consider the decay of an ST phonon of frequency much less than the Debye frequency ω_D. Then, the phase velocity v is almost independent of the magnitude of the wave vector, i.e., we can write

$$\omega(\mathbf{k}j)=v(\hat{\mathbf{k}}j)k\ . \tag{15}$$

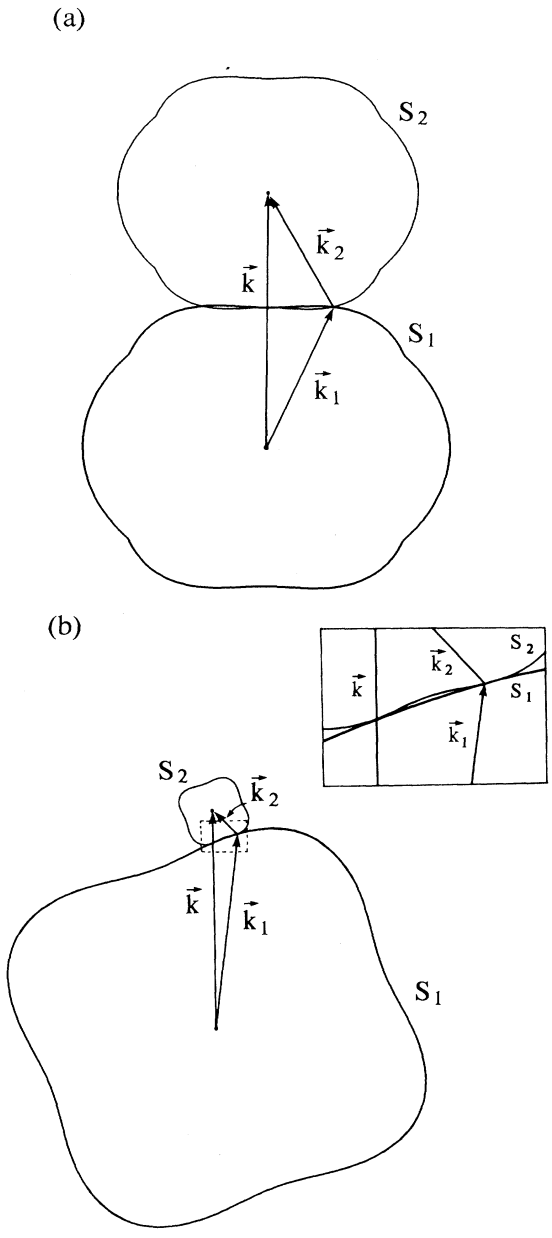

FIG. 11. Herring construction for decay of low-energy ST phonons in silicon. (a) Decay of a phonon with wave vector on a concave part of the constant frequency surface. In this example the phonon wave vector is in the [001] direction, and (110) sections of the constant-frequency surfaces for the ST phonons are shown. (b) Decay of a phonon from a convex part of the constant frequency surface. In this example the ST phonon wave vector lies in the (100) plane, and the sections of the constant-frequency surfaces lie in this plane. The inset shows an expanded view of the region enclosed by the dashed line.

For the decay of an ST phonon into two other ST phonons it then follows from Eq. (15) that the surfaces S_1 and S_2 will make tangential contact at a point where $\mathbf{k}$, $\mathbf{k}_1$, and $\mathbf{k}_2$ are all parallel. We call this point the collinear point since it corresponds to a collinear phonon decay process. However, even when $\omega \ll \omega_D$ there will be a finite but small amount of dispersion. Assuming that this dispersion is of the usual sign,[36] one finds that instead of tangential contact there is a small gap between the two surfaces, i.e., the surfaces will be as drawn in Fig. 11(a). Whether or not there will be some allowed decay processes will then depend upon whether the S_1 and S_2 surfaces intersect in places away from the collinear point (noncollinear processes).

If the CF surfaces are concave outward near the collinear point [as drawn in Fig. 11(a)] it is clear that, provided the residual effect of dispersion is not too large, there must be other intersections away from the collinear point. Since Fig. 11(a) is in fact a section through the various three-dimensional CF surfaces, a *sufficient* condition for the existence of decay modes is the existence of at least one negative principal curvature of the CF surface. Hence, ST phonons with wave vectors lying in such regions of the CF surface can never be stable excitations. In Figs. 8 and 10 we have indicated the concave and saddle regions in which at least one principal curvature is negative. One can see that, while all phonons in these regions are indeed found to be unstable, not all unstable phonons come from these regions. Thus, as stated above a negative principal curvature is a sufficient but not a necessary condition for instability.

One can see from Figs. 6 and 8 that the decay probability for ST phonons becomes very large near to the parabolic lines (zero Gaussian curvature) on the CF surfaces. The peaks of the ST phonon decay rate at $\theta = 14°$ in the (100) plane and also at $\theta = 12°$ in the (110) plane rotated away from the [001] direction occur at the zero-curvature points of the CF surface as can be seen in Fig. 8. Also the enhancement at $\theta = 60°$ in the (110) plane at the boundary occurs at the boundary between saddle and convex regions.

We have investigated these decays that occur from convex regions of the CF surface. We find that in these decay processes the energy of the starting phonon is usually divided very unequally between the two product phonons. An example of a Herring diagram for such a process is shown in Fig. 11(b). This shows the decay of an ST phonon in silicon with wave-vector direction $\theta = 20°$ and $\phi = 0°$ and the section shown is normal to the (100) plane. The original phonon is split into phonons of energy 0.14 and 0.86 of the energy of the original phonon. In geometric terms the decay of ST phonons from convex regions is possible if near to the collinear point there is a cusp on the CF surface [as in Fig. 11(b)], or a region with negative curvature. Starting from Eqs. (13) and (14) it is straightforward to show that decay of a phonon $\mathbf{k}$ into phonons $\mathbf{k}_1$ and $\mathbf{k}_2$ with $k_2 \ll k_1$ is possible if

$$\mathbf{k}_2 \cdot \mathbf{v}_g(\mathbf{k}) = v(\mathbf{k}_2) , \tag{16}$$

where $\mathbf{v}_g(\mathbf{k})$ denotes the group velocity of phonon $\mathbf{k}$.

IV. PHONON PROPAGATION WITH DECAY

A. General features

We consider a situation in which a source injects into a crystal a broad distribution of phonons, i.e., a distribution with wave vectors all across the Brillouin zone and with all polarizations. The evolution of such a distribution will be governed by the following considerations.

(1) All phonons except the part of the ST spectrum that is stable will decay into pairs of lower energy phonons. Some of the decay products will be ST in the stable region. The remainder will undergo further decays. The end point of this chain of processes is when all phonons have become either ST lying in the stable region (*S* phonons), or are of such low energy that, although in principle unstable, their lifetime is long compared to the time scale of the experiment (LE phonons). The LE phonons include ST phonons lying in the part of momentum space where this branch is unstable.

(2) As far as we can see, the largest part of the energy should end up as stable ST phonons, rather than as LE phonons. This is based upon the following considerations. Assuming that the time scale of the experiment is set by the time to propagate across a macroscopic crystal (e.g., a crystal of dimensions several centimeters) the LE phonons typically must have a frequency below about a tenth of the Debye frequency.[37] This is necessary so that their lifetime is greater than the transit time across the crystal. A high-energy phonon introduced into the crystal can therefore lead to the production of an LE phonon in one of two ways. The first possibility is that a decay process occurs in which one of the daughter phonons has a much smaller energy than the other. Thus, an LE phonon is produced in a single step. However, the probability of this is small because the majority of decays produce two phonons of roughly equal energy.[38] The second possibility is for the LE phonon to be produced after a sequence of several decays of higher energy phonons. However, as has been emphasized by Lax *et al.*,[30] in each decay at least one of the product phonons must have a smaller phase velocity than the original phonon. The phonons of smallest phase velocity are the stable ST phonons, and so the Lax condition tends to force the decays into the stable ST phonons. This argument is strengthened by a detailed analysis of the decay modes of the unstable ST phonons. This shows that the majority of decays are into *stable* ST phonons.

It is interesting to consider the effect of phonon decays on the phonon-focusing patterns.[7,39,40] In a phonon-focusing experiment phonons are injected at a point on one surface of a crystal and the intensity of phonons arriving at an opposite face is studied as a function of the position.[40] In the simplest experiment of this type the injected phonons are of low energy. Consequently, even if the phonons are allowed to decay by the conservation laws they are unlikely to actually decay while traveling across the sample. The variation of the intensity with position occurs because even if a uniform angular distribution of phonon wave vectors is generated, the angular distribution of group velocity vectors will be nonuniform

due to the crystalline anisotropy. It is found that the intensity may be very large in certain directions. The group velocity vector is normal to the constant frequency CF surfaces. Hence, in the vicinity of points on the CF surface where one of the principal curvatures changes sign there will be a large number of **k** values with almost the same direction of $\mathbf{v}_g(\mathbf{k})$. Thus, in the real space direction corresponding to the direction of this $\mathbf{v}_g(\mathbf{k})$ there will be a very large phonon intensity.

As far as we can see, such sharp features should be absent when one injects a broad distribution of phonons into a crystal at low temperature, and the phonons propagate subject only to anharmonic decay. The decays lead to a phonon distribution that consists primarily of ST phonons from the stable region of **k** space. As discussed in Sec. III C this does not include the regions of **k** space that give rise to the strong peaks in phonon intensity in the focusing directions. As the simplest possible model we assume that the distribution produced after the decays have occurred consists entirely of ST phonons in the stable region of **k** space, and we assume that in this region there are the same number of phonons for each wave vector. We consider a point source and calculate the total flux passing through a (100) plane at some distance from the source as a function of the position in the plane. For silicon the result is shown in Fig. 12. One can see that the intensity distribution is devoid of the sharp features characteristic of normal phonon-focusing experiments.[40]

B. Quasiballistics

As mentioned in the Introduction, Kazakovtsev and Levinson[7,8] have proposed that the propagation of phonons under the conditions discussed here (anharmonic decay and absence of impurity or defect scattering) could be considered in terms of a "succession of generations" model. In this theory it is assumed that high-energy phonons injected into a crystal will undergo an endless chain of decays.[41] It appears from the arguments we have given that most decay chains will, in fact, end rather quickly with the production of a number of stable ST phonons, and that the assumption on which the Kazakovtsev-Levinson theory is based is therefore incorrect.

C. Memory of source polarization

In Sec. II we discussed the way in which a recoiling atom might generate phonons in a crystal. We showed that, at least for simple crystals in which the atoms interact via a Lennard-Jones potential the primary phonons should be radiated preferentially with **k** vectors perpendicular to the recoil direction. A key question is the extent to which this anisotropy will survive the randomizing effect of the decays of these primary phonons.

Let the recoil direction be along the z axis, so that the primary phonons have wave vectors in the x-y plane. As a rough measure of the degree to which the memory of the recoil direction is retained we can consider the quantity χ defined by

$$\chi \equiv \frac{3\sum k_x^2+k_y^2}{\sum k_x^2+k_y^2+k_z^2}-2\ , \tag{17}$$

where the sums are over all phonons. For the initial distribution k_z is zero and so $\chi=1$, whereas if the directions of the wave vectors are random $\chi=0$. When a phonon decays the product phonons do not have the same propa-

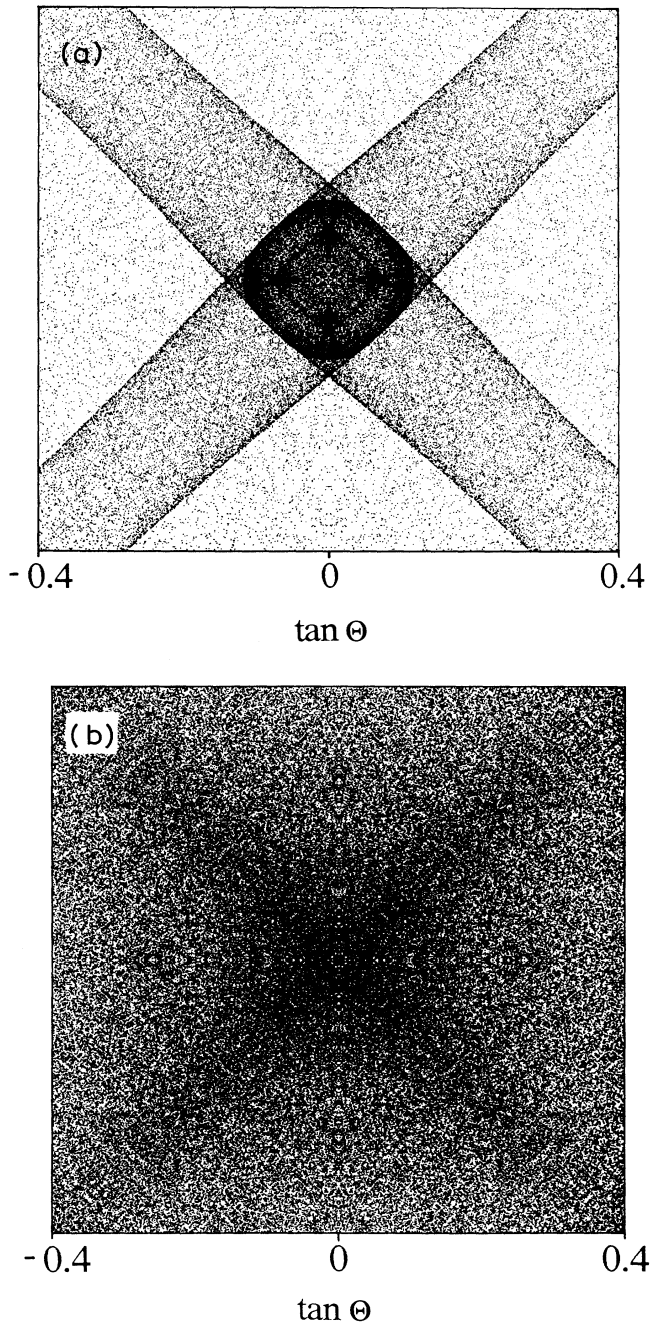

FIG. 12. Focusing pattern of low-energy ST phonons in silicon in the (100) plane for (a) a uniform distribution of wave vectors **k** space and (b) a uniform distribution of wave vectors within the stable regions. Θ is the polar angle measured from the [100] axis in real space.

gation direction as the original phonon, and so decay processes tend to lower the value of χ from its initial value. We have calculated this loss of memory on the basis of a model in which the phonons have a linear dispersion with transverse and longitudinal sound velocities v_t and v_l, respectively. In this model the transverse modes are degenerate, and so there is no loss of memory associated with the transverse phonon part of the initial phonon distribution. For typical values of v_t/v_l (i.e., ~ 0.6) the loss of memory that occurs when longitudinal phonons decay into transverse is about 50%. Thus, if equal energy goes into longitudinal and transverse phonons the loss of memory is only 25%, and so it appears that analysis of the anisotropy of the phonon flux could be used to determine the recoil direction.

For covalent crystals (Si, Ge) the situation is much less clear. One does not have an understanding of the primary phonon generation process, so the degree of anisotropy of the primary flux is not known. Simple estimates indicate that an anisotropy of the optical phonon distribution is unlikely to lead to a significant anisotropy of the final ST flux after the decay cascade is complete. However, anisotropy in the ST component of the primary phonon flux should survive.

D. Effect of isotopic impurities

These calculations assume that the elastic scattering due to isotopic mass differences can be neglected. To observe the effects we have discussed here (particularly the "memory" of the polarization of the source) the mean free path for elastic scattering of the slow transverse phonons must be at least as large as the sample dimensions.[42] For cubic crystals with one atom per unit cell, and also for Si and Ge, the phonon lifetime $\tau_{\rm iso}$ due to scattering by the variation of isotope masses can be expressed in the form[43]

$$\tau_{\rm iso}=\frac{2}{\pi\delta x\,\omega^2 g(\omega)}\ , \tag{18}$$

where $g(\omega)$ is the phonon density of states and

$$\delta x=\sum x_i\left[\frac{M_i-\overline{M}}{M}\right]^2 . \tag{19}$$

Here x_i is the fraction of isotopes that have the mass M_i and $\overline{M}$ is the average mass. It is necessary to have

$$v_t\tau_{\rm iso}\geq L\ , \tag{20}$$

where L is the linear dimensions of the sample.

Unless the crystal is composed of elements that occur naturally as a single isotope, it is difficult to satisfy condition (20). Since $g(\omega)$ is normalized to 1, the order of magnitude[44] of g is ω_D^{-1}. Suppose that there is a majority isotope of mass M and one minority isotope of concentration x and mass differing from M by one amu. Then condition (20) is equivalent to

$$x\leq\frac{8M^2v_t}{\pi L\omega_D}\ , \tag{21}$$

where we have assumed that the transverse phonons typically have a frequency of $\omega_D/2$, and M is measured in amu. v_t/ω_D is typically of the order of 1 Å, and so that condition becomes

$$x\leq 3\times 10^{-8}\frac{M^2}{L}\ . \tag{22}$$

Hence, for a silicon crystal ($M=28$ amu) of size 1 cm, x has to be less than 3×10^{-5}. Thus, a high degree of isotopic purity is required in order for the stable ST phonons to propagate ballistically.

V. SUMMARY

Dark-matter searches are currently being attempted using low-temperature phonon-based detection schemes. When a dark-matter particle scatters off a nucleus in a crystal, the recoiling nucleus will lose its energy to the lattice and high-energy phonons will be produced. These phonons will propagate away from the interaction point and the majority of them will decay into lower energy phonons before they reach the surface of the target crystal. We have investigated the extent to which the distribution of phonons searching the surface has an anisotropy that reflects the direction of recoil of the nucleus. If this phonon anisotropy exists it might be possible to use measurements of the phonon flux to deduce the direction of nuclear recoil for individual events, or at least some statistical information about the recoil distribution. This could be an important factor in the operation of a successful detector. Because of the motion of the Sun through the galaxy there should be a large anisotropy in the distribution of nuclear recoil directions such that there are many events in which nuclei recoil in the direction opposed to the motion of the Sun.[45] This anisotropy is a characteristic feature of recoil events arising from dark-matter interactions, and could be used to identify a genuine signal rate that arises from dark matter from other processes such as the internal radioactivity of the target material.

The calculation of the phonon anisotropy consists of two parts. (1) The first is a consideration of the anisotropy of the primeval phonons, i.e., those that are produced immediately after the scattering event has taken place. This part of the calculation requires a consideration of the details of the interatomic forces and the structure of the particular crystal under consideration. For close-packed monatomic crystals in which the atoms interact via a two-body potential of the Lennard-Jones form (such as the inert gas solids) we show that the phonon distribution produced by nuclear recoil is likely to have a significant degree of correlation with the recoil direction. Based upon classical molecular-dynamics simulations we find that the phonon flux should be larger in the plane perpendicular to the recoil direction than in the forward or backward directions (Sec. II). There may also be a small forward-back anisotropy. We have not attempted a detailed calculation for more complex crystals (such as Si and Ge), and without such calculations it is not clear whether a significant anisotropy in the phonon flux will exist. In Sec. III we have calculated the decay rates of

the primeval phonons in a simple model system as a function of wave vector and phonon polarization. For slow transverse phonons the decay rate was found to be zero over a large part of the Brillouin zone. We find (Sec. IV) that the decay products of high-energy phonons introduced into a crystal will primarily be slow transverse phonons with wave vectors lying in the part of the Brillouin zone where decays cannot occur. Thus, these phonons will make the major contribution to the signal seen by a phonon detector. Finally, we show that, at least in crystals with one atom per unit cell (and therefore no optical modes) the phonon distribution after the anharmonic decays have occurred retains a significant amount of memory of the anisotropy of the original phonon distribution.

ACKNOWLEDGMENTS

The authors would like to thank B. Cabrera, T. More, and B. Sadoulet for helpful discussions. This work was supported in part by the NSF through the Center for Particle Astrophysics, through DOE Grant No. DE-FG02-86ER45267, the Suhara Memorial Foundation, and the international exchange program at Hokkaido University.

---

[1]See, for example, B. Sadoulet, B. Cabrera, H. J. Maris, and J. P. Wolfe, in *PHONONS 89,* edited by S. Hunklinger, W. Ludwig, and G. Weiss (World Scientific, Singapore, 1990), p. 1383.

[2]B. Cabrera, in *PHONONS 89* (Ref. 1), p. 1373.

[3]For a short reveiw of molecular dynamics simulations of radiation damage in crystals, see D. N. Seidman, R. S. Averback, and R. Benedek, Phys. Status Solidi **144**, 85 (1987).

[4]The only exceptions are some of the slow transverse (ST) phonons. The range of wave vectors for these stable phonons is calculated in Sec. III C.

[5]For example, in silicon the time for the average phonon enegy to decrease to 0.1 K via anharmonic processes is of the order of 1 year; see H. J. Maris, Phys. Rev. B **41**, 9736 (1990).

[6]G. L. Slonimskii, Zh. Eksp. Teor. Fiz. **7**, 1457 (1937).

[7]D. V. Kazakovtsev and Y. B. Levinson, Pis'ma Zh. Eksp. Teor. Fiz. **27**, 181 (1978) [JETP Lett. **27**, 169 (1978)].

[8]Y. B. Levinson, in *Nonequilibrium Phonons in Nonmetallic Crystals,* edited by W. Eisenmenger and A. A. Kaplyanski (North-Holland, Amsterdam, 1986), pp. 91–143.

[9]See Ref. 8, p. 122.

[10]B. Taylor, H. J. Maris, and C. Elbaum, Phys. Rev. Lett. **23**, 416 (1969); Phys. Rev. B **3**, 1462 (1971).

[11]J. R. Primack, D. Seckel, and B. Sadoulet, Ann. Rev. Nucl. Part. Sci. **38**, 751 (1988).

[12]F. W. Clinard and L. W Hobbs, in *Physics of Radiation Effects in Crystals,* edited by R. A. Johnson and A. N. Orlov (North-Holland, Amsterdam, 1986), p. 392.

[13]This discussion assumes that the majority of the recoil energy goes into phonon production, and not into ionization.

[14]This result can be derived using the expressions connecting the normal mode coordinates and the momentum and displacement of atoms in a crystal lattice which are given in A. A. Maradudin, E. W. Montroll, and G. H. Weiss, *Lattice Dynamics in the Harmonic Approximation* (Academic, New York, 1963), Chap. 2.

[15]For some studies of solitons in Lennard-Jones chains, see F. Yoshida and T. Sakuma, Prog. Theor. Phys. **61**, 676 (1979); Y. Ishimori, *ibid* **68**, 402 (1982); M. A. Collins and S. A. Rice, J. Chem. Phys. **77**, 2607 (1982); L. Solheim and M. K. Ali, Prog. Theor. Phys. **71**, 487 (1984).

[16]For recent work on silicon, see A. M. Mazzone, Nucl. Instrum. Methods **B18**, 253 (1987); **B33**, 776 (1988).

[17]The interatomic potential in silicon has been discussed recently by E. Kaxiras and K. C. Pandey, Phys. Rev. B **38**, 12 736 (1988).

[18]These excitations are the same as the "focusons" originally discussed by R. H. Silsbee, J. Appl. Phys. **28**, 1246 (1957).

[19]These are dimensionless recoil velocities in the approximate numerical range relevant to dark-matter experiments.

[20]For a discussion of the Lennard-Jones potential, see C. Kittel *Introduction to Solid State Physics* (Wiley, New York, 1971), Chap. 3.

[21]P. F. Smith and J. D. Lewin, Phys. Rep. **187**, 203 (1990).

[22]A. A. Maradudin, P. A. Flinn, and R. A. Coldwell-Horsfall, Ann. Phys. (N.Y.) **15**, 360 (1961).

[23]A. A. Maradudin and A. E. Fein, Phys. Rev. **128**, 2589 (1962); A. A. Maradudin, A. E. Fein, and G. H. Vineyard, Phys. Status Solidi **2**, 1479 (1962).

[24]The values of γ for LiF, NaF, Si, and Ge were estimated from the data reported in H. R. Shanks, P. D. Maycock, P. H. Sidles, and G. C. Danielson, Phys. Rev. **130**, 1743 (1963); H. Ibach, Phys. Status Solidi **31**, 265 (1969); T. H. K. Barron, J. G. Collins, and G. K. White, Adv. Phys. **29**, 609 (1980); γ for Ne, Ar, Kr, and Xe is discussed by P. Korpiun and E. Löscher, in *Rare Gas Solids,* edited by M. L. Klein and J. A. Venables (Academic, New York, 1976), p. 816.

[25]The results were obtained with a modification of the Brillouin zone-integration method originally devised by G. Gilat and L. J. Raubenheimer [Phys. Rev. **144**, 390 (1966)] for the calculation of the one-phonon density of states. In the application of this method to the calculation of the decay rate for $\mathbf{k}j \rightarrow \mathbf{k}_1 j_1 + \mathbf{k}_2 j_2$ the first Brillouin zone of $\mathbf{k}_1$ is divided into small cubic cells with sides of length π/na, where a is the lattice constant and n is typically 30–40. One then finds those cubic cells within which there is a section of the surface on which the quantity $\omega(\mathbf{k}j)-\omega(\mathbf{k}_1 j_1)-\omega(\mathbf{k}-\mathbf{k}_1 j_2)$ vanishes. To obtain the contribution to the decay rate from a particular cell one then makes a linear approximation to the variations of $\omega(\mathbf{k}_1 j_1)$ and $\omega(\mathbf{k}-\mathbf{k}_1 j_2)$ with $\mathbf{k}_1$ so that the integral over the cell can be evaluated. The matrix element of the anharmonic potential is taken to be constant throughout each cell.

[26]The strong enhancement of the decay rate for longitudinal phonons near to the X point occurs because these phonons have a very large number of possible decay products. This is a special feature of the dispersion relation for phonons in the fcc lattice with nearest-neighbor central forces, and is unlikely to occur in real crystals.

[27]C. Herring, Phys. Rev. **95**, 954 (1954).

[28]R. Orbach and L. A. Vredevoe, Physics **1**, 91 (1964).

[29]H. J. Maris, Phys. Lett. **17**, 228 (1965). In this paper the range of wave vectors of the ST phonons that cannot decay was es-

timated using a very coarse mesh of points in **k** space. Consequently, some fine details of the range were missed in this calculation. For example, the fact that phonons with small wave vectors near to the ⟨111⟩ directions can decay was missed.

[30]M. Lax, P. Hu, and V. Narayanamurti, Phys. Rev. B **23**, 3095 (1981).

[31]S. Tamura and H. J. Maris, Phys. Rev. B **31**, 2595 (1985).

[32]A. Berke, A. P. Mayer, and R. K. Wehner, J. Phys. C **21**, 2305 (1988).

[33]S. Narasimhan and D. Vanderbilt, Phys. Rev. B **43**, 4541 (1991).

[34]S. Tamura, J. A. Shields, and J. P. Wolfe, Phys. Rev. B **44**, 3001 (1991).

[35]If the optical frequencies are higher than this, it may still be possible for the optical phonons to decay by a higher-order process.

[36]By the "usual sign," we mean that it is of the same type as occurs in a linear chain of particles interacting via nearest-neighbor forces.

[37]This follows from the results shown in Fig. 5, together with the parameters listed in Table I. The decay rate has to be less than about $10^6\ s^{-1}$.

[38]M. T. Labrot, A. P. Mayer, and R. K. Wehner, J. Phys. C **1**, 8809 (1989).

[39]H. J. Maris, J. Acoust. Soc. Am. **50**, 812 (1971).

[40]For a review of recent experimental work, see J. P. Wolfe, in *PHONONS 89* (Ref. 1), p. 1335.

[41]See, for example, p. 121 of Ref. 8.

[42]Note that this is a *much* stronger condition than the requirement that the elastic scattering rate be less than the anharmonic decay rate for phonons that are allowed to decay.

[43]See, for example, H. J. Maris, Philos. Mag. **13**, 465 (1966).

[44]There is usually a peak in the density of states in the range near to the highest frequency of the ST phonon spectrum. Consequently, the order of magnitude estimate we have given of the density of states is probably somewhat too low.

[45]The anisotropy is calculated by D. N. Spergel, Phys. Rev. D **37**, 1353 (1988).